Theoretical Notes
Note 194

SLA-73-0338

CALCULATION OF SPECTRA FROM EMP-TYPE WAVEFORMS

Charles N. Vittitoe

Theoretical Division
Simulation Sciences Research Department
Sandia Laboratories
Albuquerque, New Mexico
87115

March 1973

ABSTRACT

Electromagnetic pulses typically have a large amplitude over a very small time interval. As a result, a substantial portion of their spectra is at high frequencies. Lower frequency contributions then occur for times several orders of magnitude larger. A method is presented for calculating the Fourier transform of such pulses. This procedure may improve the high-frequency representation in cases where $|F(\omega)| \sim \omega^n$ with $n \geq -4$ at high frequencies. Limitations are discussed, together with those of the usual transform methods. Two examples are used as illustrations.

Key Words: Electromagnetic Pulse, Fourier Transform

Intentionally Left Blank

TABLE OF CONTENTS

Intentionally Left Blank

CALCULATION OF SPECTRA FROM EMP-TYPE WAVEFORMS

Introduction

Volumes have been written concerning the interaction of electromagnetic fields with antennae. In nearly every case, actual calculations are done in the frequency domain rather than in the time domain. The recent EMP Handbook[1] illustrates several of the most popular methods. The connection between the two domains is the familiar Fourier transform pair,

$$F(\omega) = \int_{-\infty}^{\infty} f(t)\ e^{-i\omega t}\ dt \qquad (1)$$

and

$$f(t) = \frac{1}{2\pi} \int_{-\infty}^{\infty} F(\omega)\ e^{i\omega t}\ d\omega \quad . \qquad (2)$$

In EMP studies, real causal signals are expected; hence, the $f(t)$ is real and is zero for t less than the time of signal arrival, t_a. Because of the rapid rise of the leading edge of the EMP, t_a is difficult to determine accurately in many applications. Usually the initial time is chosen sufficiently early that the $F(\omega)$ results are not affected (i.e., the amplitude $f(t)$ is small enough for $t < t_a$ that the integral for $F(\omega)$ is not affected).

Equation (1) appears extremely easy to solve, especially in this day of high-speed computers. An approach which comes quickly to mind

is to separate the time axis into intervals, choose a representative amplitude for each interval, multiply the appropriate factors together, and sum over all the intervals. As the intervals are made smaller, the summation should converge to the proper transform. Such a numerical treatment is unsatisfactory because of discontinuities in f(t). If we assume that f(t) is an entire function over $(-\infty, \infty)$, the artificial discontinuities in f(t) (introduced by the numerical technique) prevent accurate representation of $F(\omega)$ at large ω. If the first n-1 derivatives of f(t) are continuous, then integration by parts (subject to the usual restrictions that the function and all its derivatives vanish at the integration limits) gives[2]

$$F(\omega) = \frac{1}{(i\omega)^{\eta}} \int_{-\infty}^{\infty} f^{\eta}(t)\, e^{-i\omega t}\, dt \quad . \tag{3}$$

If the specific f(t) had a transform such that

$$|F(\omega)| \sim 1/\omega^{\eta_1}$$

at large ω, the numerical procedure described earlier could not accurately represent $|F(\omega)|$ for $\eta_1 > 1$.

For high frequencies there is a second difficulty with this simple approach. With a given time interval size, Δt, at high frequencies the phase factor $-i\omega t$ will change significantly as time proceeds across the interval. No unique phase factor may be chosen as representative of the interval. With a given f(t), the time intervals may be chosen sufficiently small to overcome this difficulty, i.e., provided the frequencies of interest are not too large. If constant interval spacing is also

specified, the fast Fourier transform algorithm may be used.[3] Consider a situation where $F(\omega)$ is desired for $\omega \leq \pi \times 10^9$ sec^{-1}. The time interval necessary is then limited by

$$\Delta t \leq \pi/\omega_{max} = 10^{-9} \text{sec}.$$

If $f(t)$ is significant for times near 100 μsec, then 10^5 intervals must be considered if Δt is to remain constant. Such storage is near the limit of some modern computers. With 10^5 terms, the standard transform methods also cease to be rapid, especially if a sufficient number of data points is not readily available.

Carpenter and Price[5] have suggested a method which solves the storage difficulties and the representative phase choice for the intervals. They approximate $f(t)$ by a series of straight-line segments with sections of the function having constant Δt. Thus when the function is rapidly varying, a small Δt is used. At later times when $f(t)$ is slowly varying, larger interval sizes are allowed. This approach solves the storage problem for many applications. They also calculate the special transition terms[5] required when the interval size is changed. The choice of straight-line segments allows them to include the variation of phase across the interval. However, such a method gives discontinuities in the numerical representation of the first derivative of $f(t)$. Any $|F(\omega)|$ which falls faster than $1/\omega^2$ cannot be accurate at large ω. The numerical procedure has forced a ω^{-2} dependence at large ω.

An additional concern with the fast Fourier transform technique is the basic assumption that the wave is periodic with a period equal to the time interval chosen for the integration. Transformation back into

the time domain with account taken of response functions often yields a leading edge to the waveform that corresponds to the "preceding" pulse.

The high-frequency behavior of $F(\omega)$ is important in many applications concerning the interaction of an electromagnetic pulse with systems. Many systems have antennae on the order of one meter long. Assuming half wavelength resonance, $\omega \approx 3\pi \times 10^8$ sec^{-1} will couple strongly with the antenna. In other applications, still higher frequencies may be important.

Spline Fitting Technique and Resultant Transform*

A spline fitting technique can be used to represent the function f(t).[4] The derivatives $f^n(t)$ can be represented by continuous functions by the choice of an n+1-order spline. A cubic spline, for example, could represent a continuous f(t) with continuous first and second derivatives. Because of the numerical procedure in the frequency domain the discontinuous third derivative would force $|F(\omega)|$ to fall as $1/\omega^{n_1}$ with $n_1 = 4$. Thus, accurate high-frequency representation is possible for larger n_1.

A cubic spline representation of f(t) is written

$$f(t) = \alpha_1 + \alpha_2 t + \alpha_3 t^2 + \alpha_4 t^3 + \sum_{j=5}^{K} \alpha_j (t-\beta_j)_+^3 \quad , \qquad (4a)$$

where $(x)_+ = xh(x)$ and h(x) is the Heaviside unit step function. The joints, β_j, are distributed along the t axis with special attention to times at extrema of f(t) or where slopes are rapidly changing. The coefficients α_j are then determined by a fitting procedure described elsewhere.[4] The β_j may be varied to improve the fit.[4]

In order to calculate $F(\omega)$, the f(t) must be specified for all time. Because of difficulty in precise determination of the time of arrival t_a, the f(t) is represented by

$$f(t) = \alpha_{oA} \exp(\alpha_o t) \qquad (4b)$$

for $t < t_o$. Rather than following f(t) to $t = \infty$, it is represented by

$$f(t) = \alpha_{\infty A} \exp(-\alpha_\infty t) \qquad (4c)$$

for $t > t_\infty$. The spline fit is then required in the interval $t_o \le t \le t_\infty$.

---

*Private communication with J. N. Wood of Science Applications, Inc., Dec. 1972, indicates that the Air Force Weapons Laboratory has been using a version of spline fitting to transform the t, E(t) data generated by some of their electromagnetic pulse programs.

The new parameters must be adjusted to keep continuous first and second derivatives in the interval $-\infty \le t \le \infty$. The choices of t_o and t_∞ can be varied to insure that the end functions contribute only a small amount to the transform. If other information concerning the late time behavior is available (such as a damped sinusoidal form) the end functions might be improved for some applications.

In order to insure equality of the function and its first derivative at the transition points, the following constraints are placed on the coefficients:

$$\alpha_o = \frac{\alpha_2+2\alpha_3 t_o+3\alpha_4 t_o^2}{\alpha_1+\alpha_2 t_o+\alpha_3 t_o^2+\alpha_4 t_o^3} \quad ,$$

$$\alpha_{oA} = e^{-\alpha_o t_o}\left\{\alpha_1 + \alpha_2 t_o + \alpha_3 t_o^2 + \alpha_4 t_o^3\right\} \quad ,$$

$$-\alpha_\infty = \frac{\alpha_2+2\alpha_3 t_\infty+3\alpha_4 t_\infty^2+\sum_{j=5}^{K} 3\alpha_j(t_\infty-\beta_j)^2}{\alpha_1+\alpha_2 t_\infty+\alpha_3 t_\infty^2+\alpha_4 t_\infty^3+\sum_{j=5}^{K} \alpha_j(t_\infty-\beta_j)^3} \quad , \tag{5}$$

$$\alpha_{\infty A} = e^{\alpha_\infty t_\infty}\left\{\alpha_1 + \alpha_2 t_\infty + \alpha_3 t_\infty^2 + \alpha_4 t_\infty^3 + \sum_{j=5}^{K}\alpha_j(t_\infty-\beta_j)^3\right\} .$$

In order to insure continuity of the second derivative at t_o and t_∞, the second derivative in the spline fit is constrained to be

$$f^{(2)}(t_o) = \alpha_o^2 f(t_o) \quad ,$$

$$f^{(2)}(t_\infty) = \alpha_\infty^2 f(t_\infty) \quad .$$

The spline-fitting routine is quite capable of applying constraints to its fitting parameters; in fact, constraints of this type are easily included.[4] The first joint (β_5) is often chosen close to t_o, with t_o

sufficiently early that the amplitude of f(t) is insignificant. Such a choice has been found helpful in efficient solution for a good fit to the data in the examples considered later.

The accuracy of the fit can always be adjusted to fit the needs of a specific problem. It can be constrained to be within some multiple (such as 10^{-3} or 10^{-6}) of each value of f(t) used to determine the fit. If the multiple is small, more joints may be required to find a suitable fit.

The transform of Eq. (4) may now be written

$$F(\omega) = \frac{\alpha_{oA}\exp(\alpha_o t_o - i\omega t_o)}{\alpha_o - i\omega} + \frac{\alpha_{\infty A}\exp[-(\alpha_\infty + i\omega)t_\infty]}{\alpha_\infty + i\omega}$$

$$+ \alpha_1\left[\chi_{t_\infty} - \chi_{t_o}\right] + \alpha_2\left[\chi_{t_\infty}\eta_{t_\infty} - \chi_{t_o}\eta_{t_o}\right]$$

$$+ \alpha_3\left[\chi_{t_\infty}\left\{t_\infty^2 + \frac{2}{i\omega}\eta_{t_\infty}\right\} - \chi_{t_o}\left\{t_o^2 + \frac{2}{i\omega}\eta_{t_o}\right\}\right] \qquad (6)$$

$$+ \alpha_4\left[\chi_{t_\infty}\left\{t_\infty^3 + \frac{3}{i\omega}t_\infty^2 - \frac{6}{\omega^2}\eta_{t_\infty}\right\} - \chi_{t_o}\left\{t_o^3 + \frac{3}{i\omega}t_o^2 - \frac{6}{\omega^2}\eta_{t_o}\right\}\right]$$

$$+ \sum_{j=5}^{K}\alpha_j\left[\chi_{t_\infty}\left\{(t_\infty-\beta_j)^3 + \frac{3}{i\omega}(t_\infty-\beta_j)^2 - \frac{6}{\omega^2}\eta_{t_\infty-\beta_j}\right\} + \chi_{\beta_j}\frac{6}{i\omega^3}\right],$$

where

$$\chi_t \equiv \frac{1}{-i\omega}\exp(-i\omega t) ,$$

$$\eta_t \equiv t + \frac{1}{i\omega} .$$

The procedure for calculating the transform can be simplified somewhat by use of Eq. (3). Since the mathematical representation of the function and its first two derivatives are all continuous,

$$F(\omega) = \frac{1}{(i\omega)^3} \int_{-\infty}^{\infty} f^{(3)}(t)\, e^{-i\omega t}\, dt \quad . \qquad (7)$$

Direct substitution gives

$$F(\omega) = \frac{\alpha_o^3 \alpha_{oA} \exp[(\alpha_o - i\omega)t_o]}{(i\omega)^3 (\alpha_o - i\omega)} - \frac{\alpha_\infty^3 \alpha_{\infty A} \exp[-(\alpha_\infty + i\omega)t_\infty]}{(i\omega)^3 (\alpha_\infty + i\omega)}$$

$$+ \frac{6\alpha_4}{(i\omega)^4} \left(e^{-i\omega t_o} - e^{-i\omega t_\infty} \right) + \sum_{j=5}^{K} \frac{6\alpha_j}{(i\omega)^4} \left(e^{-i\omega \beta_j} - e^{i\omega t_\infty} \right) \quad . \qquad (8)$$

Fluor Function Example

Let us now apply the technique to a function with typical EMP behavior for which the exact transform can be easily calculated. The fluor function

$$f_1(t) = e^{-\alpha t} - e^{-\beta t} \qquad (9)$$

fits these criteria. If $\beta \gg \alpha$, then at late times $f(t) \sim e^{-\alpha t}$, while at early times $f(t) \sim (\beta - \alpha)t$. The peak occurs at

$$t_p = \frac{1}{\beta - \alpha} \ell n(\beta/\alpha) \quad .$$

With the end functions introduced earlier, the exact Fourier transform is found to be

$$F_1(\omega) = \frac{\alpha_{oA} \exp(\alpha_o t_o - i\omega t_o)}{\alpha_o - i\omega} + \frac{\alpha_{\infty A} \exp[-(\alpha_\infty + i\omega)t_\infty]}{\alpha_\infty + i\omega}$$

$$+ \frac{\exp[-(\alpha + i\omega)t_o] - \exp[-(\alpha + i\omega)t_\infty]}{\alpha + i\omega} \qquad (10)$$

$$+ \frac{\exp[-(\beta + i\omega)t_\infty] - \exp[-(\beta + i\omega)t_o]}{\beta + i\omega} \quad .$$

The following choices were made for the input function parameters:

$$t_o = 1. \times 10^{-9},$$

$$t_\infty = 5 \times 10^{-7},$$

$$\alpha_o = 8.1103397 \times 10^{8},$$

$$\alpha_\infty = 4 \times 10^{6},$$

$$\alpha = 4 \times 10^{6},$$

$$\beta = 4 \times 10^{8},$$

with all variables in cgs-Gaussian units. Forty-three values of t such that $1 \times 10^{-9} \leq t \leq 500 \times 10^{-9}$ were chosen in order to obtain a set of data points $[t_i, f_1(t_i)]$ for use in the fitting program. The data points and the resulting fit are shown in Fig. (1). The fit coefficients (α_i), joints (β_i), fit interval (t_o, t_∞), plot interval, beginning exponential parameters (α_{oA}, α_o), and end exponential parameters ($\alpha_{\infty A}$, α_∞) are given in Table I. Several derivatives of f(t) are given in Fig. 2. Note the discontinuities that occur in the third derivative.

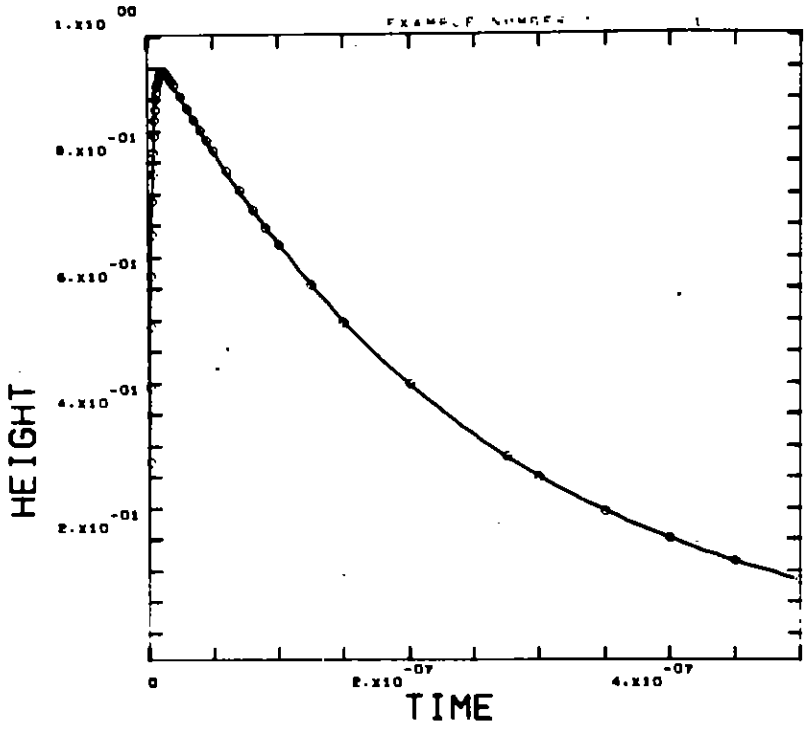

Fig. 1. Spline fit to the fluor function with end adjustments. Circles indicate data points.

7.5403722710259E-01	-1.7086686661282E+09	1.8650061667854E+18
-5.8612097037574E+26	5.9920358793626E+26	-1.0155882254916E+25
-2.5666865131857E+24	-3.6438964781629E+23	5.2219793504439E+21
-9.2895277539162E+20	4.8111284117112E+19	-6.1432700933183E+18
3.9611300328393E+18	1.1268178262603E+18	

1.0000000000000E-09	2.0000000000000E-09	5.0000000000000E-09
1.2000000000000E-08	1.8000000000000E-08	4.0000000000000E-08
9.0000000000000E-08	1.5000000000000E-07	2.5000000000000E-07
4.0000000000000E-07		

FIT INTERVAL TOO= 1.0000000000000E-09 TINE= 5.0000000000000E-07

PLOT INTERVAL TB= 0. TF= 1.0000000000000E-06

BEGINNING EXPONENTIAL PARAMETERS = 1.4409781068814E-01 8.1103397000000E+08

END EXPONENTIAL PARAMETERS 9.9988640851571E-01 4.0000000000000E+06

Table I. Fit parameters

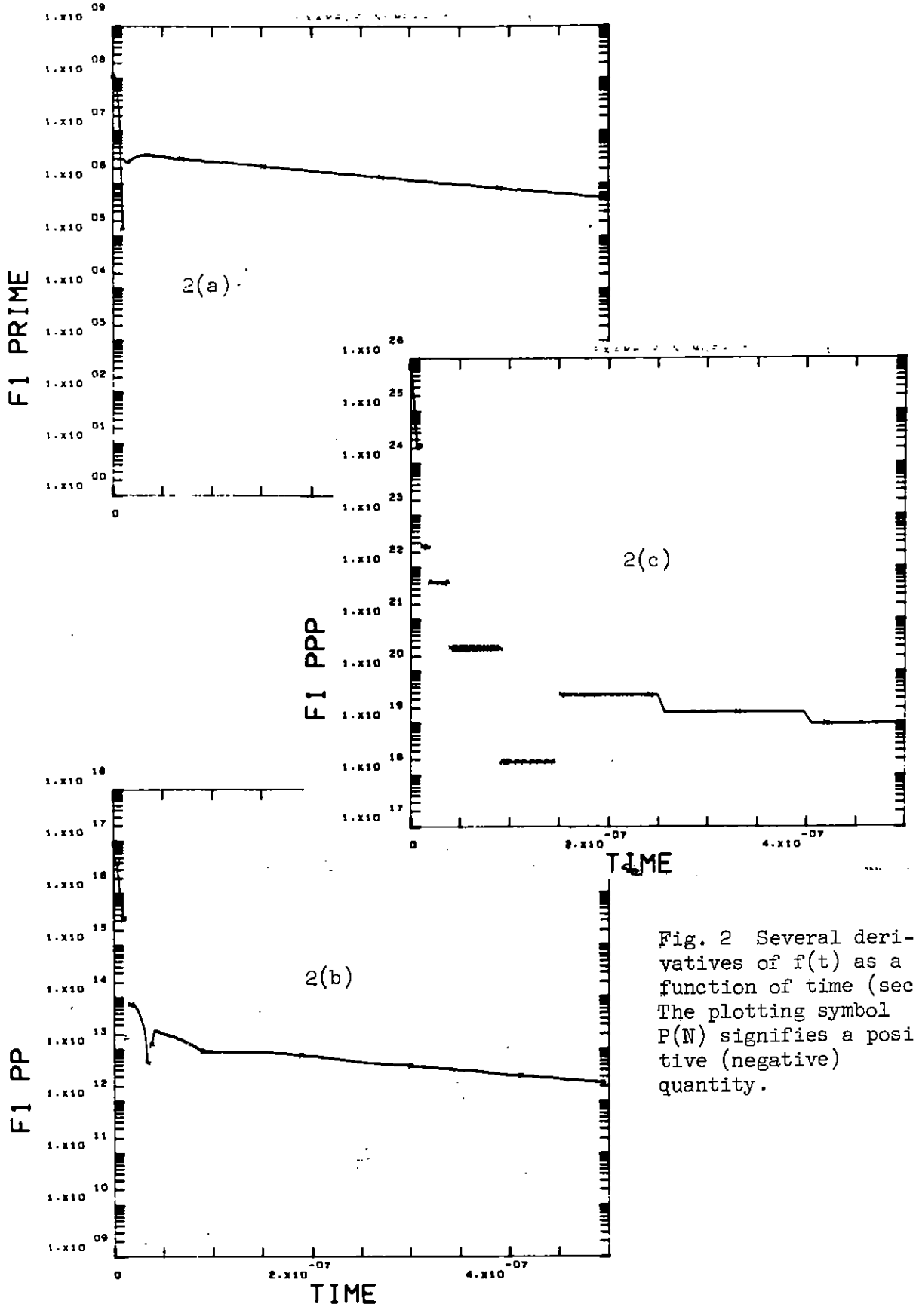

Fig. 2 Several derivatives of f(t) as a function of time (sec). The plotting symbol P(N) signifies a positive (negative) quantity.

Computer evaluation of the transform from Eq. (8) yields Fig. 3. Evaluation of the transform from Eq. (6) yields very similar results. At high frequencies the representation is reasonable. However, at angular frequencies below 2×10^5 sec^{-1} (3×10^6 sec^{-1}) the real (imaginary) part of the transform differs significantly from the exact solution. Such difficulties might be expected from computer evaluations of such quantities as $\exp(-i\omega\beta_i) - \exp(-i\omega t_\infty)$. When the arguments are small ($2 \times 10^5 \times t_\infty = 10^{-1}$; $e^{0.1} = 1.1$) the exponential functions are near 1. Significant figures are then lost when differences are taken in the computer.

Treatment at Small ω

To overcome the difficulty at small ω, Gaussian integration may be used instead of Eq. (6) when $\omega t_\infty < 2$. The equation then becomes

$$F(\omega) = \frac{\alpha_{oA} \exp[(\alpha_o - i\omega)t_o]}{\alpha_o - i\omega} + \frac{\alpha_\infty A \exp[-(\alpha_\infty + i\omega)t_\infty}{\alpha_\infty + i\omega} + \int_{t_o}^{t_\infty} f(t)\, e^{-i\omega t} dt \,, \quad (11)$$

where

$$\int_{t_o}^{t_\infty} f(t)\, e^{-i\omega t}\, dt = \sum_{\ell=1}^{N_G} w_\ell\, f(y_\ell)\, \frac{t_\infty - t_o}{2} \,,$$

$$y_\ell = \frac{t_\infty - t_o}{2} x_\ell + \frac{t_\infty - t_o}{2} \,,$$

and x_ℓ, w_ℓ are the position and weight functions for the Gaussian integration.[6] N_G is the number of points used in the integration scheme. With $N_G = 32$ and the f(t) evaluated from the spline fit, the transform is given in Fig. 4. The transform coincides well with the exact solution in Fig. 4. The time required to calculate the 51 transform points in Fig. 4 was less than 0.4 sec on a

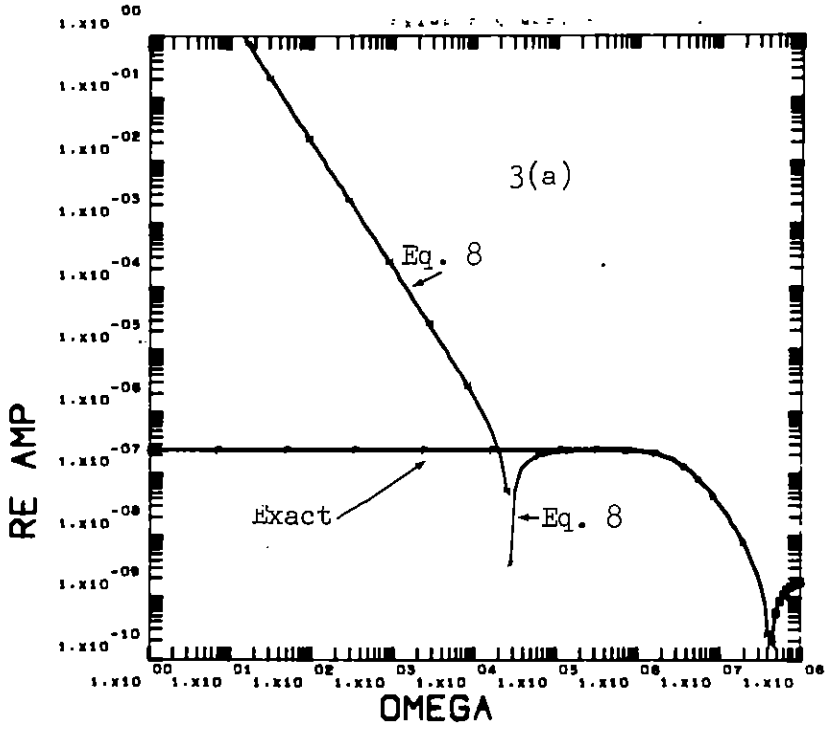

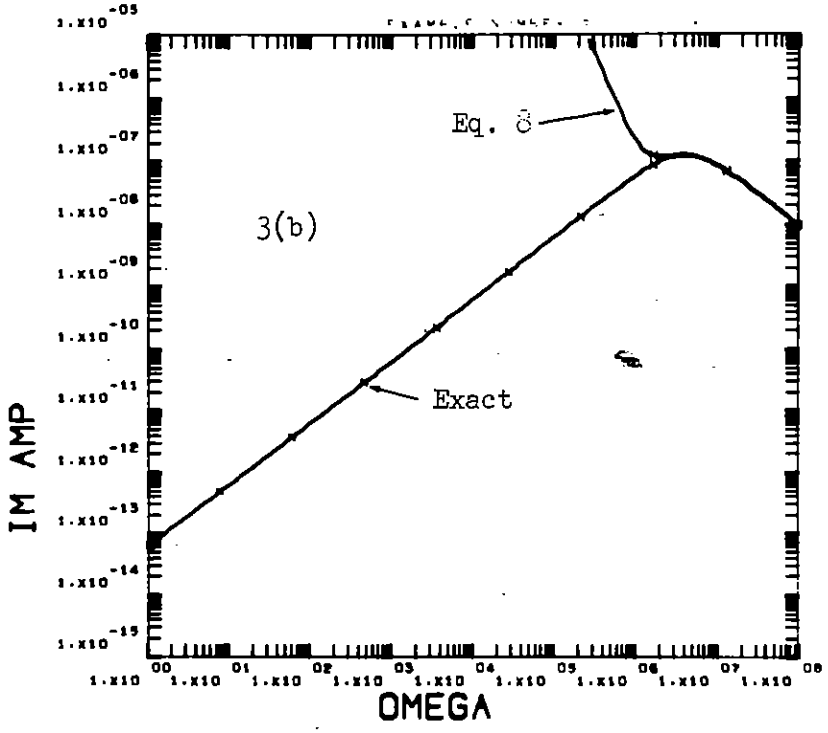

Fig. 3. Real and imaginary parts of $F(\omega)$ vs. $\omega(\text{sec}^{-1})$ for Example 1 evaluated from Eq. (8).

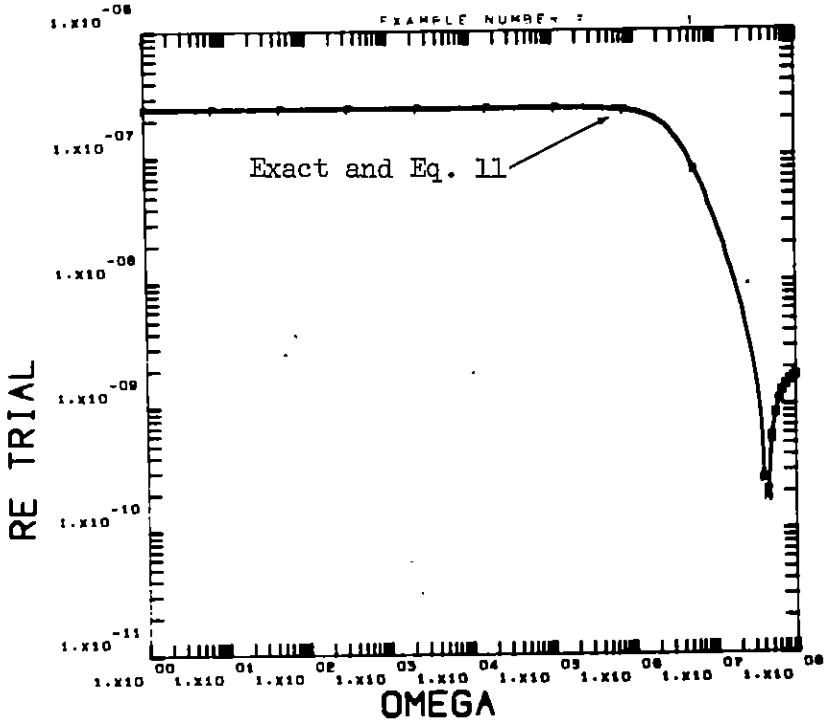

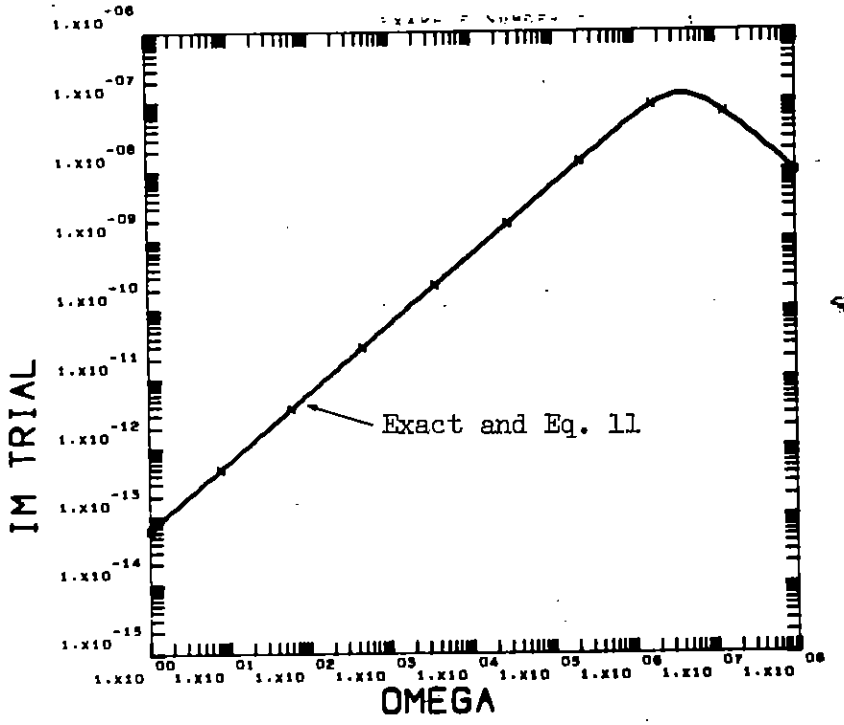

Fig. 4

Real and imaginary parts of $F(\omega)$ for Example 1 via Gaussian integration.

CDC 6600 computer, using the FTN compiler. $N_G = 8$ essentially reproduces the results in Fig. 4, and gives agreement with the exact solution within 10%.

A basic difficulty with such transforms at low frequencies has been pointed out by Higgins.[7] In Eqs. (6) and (8) terms proportional to ω^{-m} occur, with m varying from 1 to 4. Since $F(\omega = 0)$ is the finite integral of $f(t)$ over time, these ω^{-m} terms must have zero coefficients. Power series expansion of Eq. (8) indeed verifies that these terms are zero. In expansion form, the transform is given by

$$F(\omega) = \int_{-\infty}^{\infty} f(t)dt + f(t_o)\left\{\frac{\Omega_1(\frac{i\omega}{\alpha_o})}{\alpha_o}\left[1 + H_1(i\omega t_o)\right] + G(\alpha_o, t_o)\right\}$$

$$- f(t_\infty)\left\{\frac{-\Omega_1(\frac{-i\omega}{\alpha_\infty})}{\alpha_\infty}\left[1 + H_1(i\omega t_\infty)\right] + G(-\alpha_\infty, t_\infty)\right\} \qquad (12)$$

$$- \sum_{j=4}^{K} 6\alpha_j \, H_5(\omega, t_\infty) + 6\alpha_4 \, H_5(\omega, t_o) + \sum_{j=5}^{K} 6\alpha_j \, H_5(\omega, \beta_i),$$

where

$$G(\alpha,t) \equiv \frac{H_1(\omega,t)}{\alpha} + H_2(\omega,t) + \alpha H_3(\omega,t) + \alpha^2 H_4(\omega,t) \quad ,$$

$$H_\ell(\omega,t) \equiv \sum_{n=\ell}^{\infty} \frac{(-i\omega t)^{n-\ell+1}}{n!} (-t)^{\ell-1} \quad , \qquad (13)$$

$$\Omega_\ell(z) \equiv \sum_{n=\ell}^{\infty} z^n \quad .$$

If α is sufficiently small, then for $\ell = 1$ the following may be more convenient:

$$\Omega_1(\frac{i\omega}{\alpha}) = \frac{1}{1 - \frac{i\omega}{\alpha}} - 1 \quad .$$

Thus at high frequencies the transform is evaluated by Eq. (8). At low frequencies, Eq. (11) with Gaussian integration or Eq. (12) may be used.

The H_ℓ series converge quickly for $\omega t \leq 1.5$, hence only ten terms are sufficient in the series. Fig. 5 gives the transform for the fluor function example, evaluated by Eq. (12) below $\omega = 3 \times 10^6$ sec^{-1}.

A Second Example

Note that at large ω the $F_1(\omega)$ in Eq. (10) falls as $1/\omega$. Hence the fluor function is not an optimum choice for illustration that the spline-fitting procedure has advantages at large ω over methods where the first derivative of $f(t)$ is treated as discontinuous. As a better test consider the function

$$f_2(t) = \frac{t^4 \exp[-\gamma t]}{f_{2m}}$$

for $t_o \leq t \leq t_\infty$ where $f_{2m} = e^{-4}(\frac{4}{\gamma})^4$. Including the earlier end terms gives the transform

$$F(\omega) = \frac{\alpha_{oA} \exp[(\alpha_o - i\omega)t]}{\alpha_o - i\omega} + \frac{\alpha_{\infty A} \exp[-(\alpha_\infty + i\omega)t]}{\alpha_\infty + i\omega}$$

$$+ \xi_4(t_\infty) - \xi_4(t_o) + 4\nu[\xi_3(t_\infty) - \xi_3(t_o)]$$

$$+ 12\nu^2[\xi_2(t_\infty) - \xi_2(t_o)] + 24\nu^3[\xi_1(t_\infty) - \xi_1(t_o)] \qquad (15)$$

$$+ 24\nu^4[\xi_o(t_\infty) - \xi_o(t_o)] \quad ,$$

where

$$\xi_n(t) \equiv t^n \frac{\exp[-(\gamma + i\omega)t]}{-f_{2m}(\gamma + i\omega)} \quad ,$$

$$\nu \equiv \frac{1}{\gamma + i\omega} \quad .$$

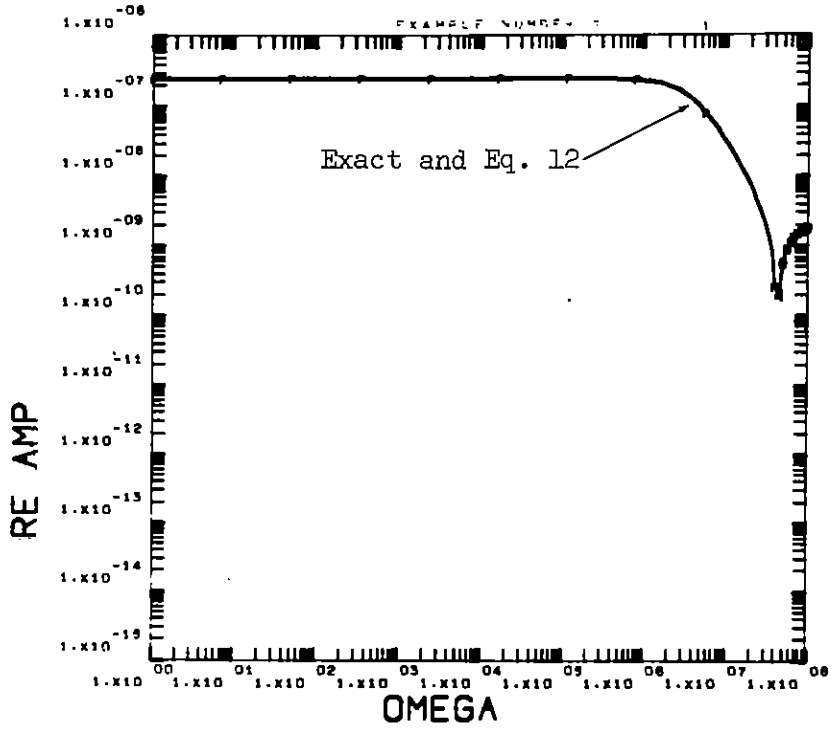

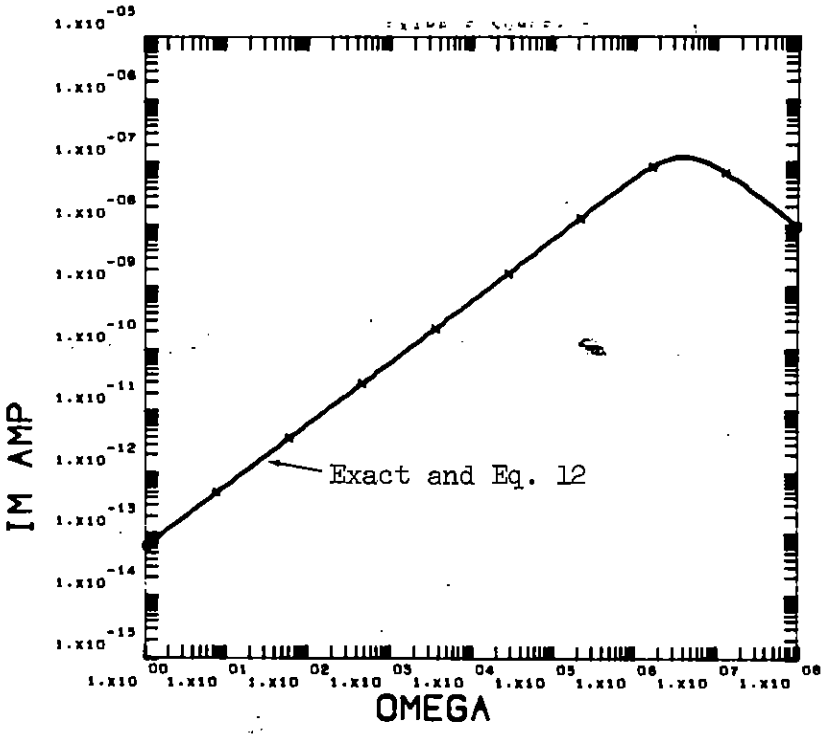

Fig. 5

Real and imaginary parts of $F(\omega)$ evaluated with aid of Eq. (12).

The following choices were made for input parameters:

$$t_o = 1. \times 10^{-9} ,$$

$$t_\infty = 5. \times 10^{-7} ,$$

$$\alpha_o = 3.96 \times 10^{9},$$

$$\alpha_\infty = 3.20 \times 10^{7},$$

$$\gamma = 4.00 \times 10^{7}.$$

The coefficients α_o and α_∞ are calculated from the value of γ and the derivatives of $f_2(t)$. Additional input used in the fitting routine were:

1. Forty-three data points giving $f_2(t)$ for $t_o \leq t \leq t_\infty$.
2. Reliability of each $f_2(t)$ value ($\pm$ 4 percent).
3. Constraint on the continuity of f_2 and its first two derivatives at t_o and t_∞.
4. Constraint on the first derivative of $f_2(t)$ to be positive at 2, 3, 4, and 6 x 10^{-8} seconds.

Table II gives the problem parameters, while the fit is illustrated in Fig. 6. Several derivatives are shown in Fig. 7.

TABLE II. Example 2 problem parameters

COEFFICIENTS

5.871172414347 2E-05	-1.08802649155 22E+05	1.06566412941 13E+14
-5.41507969101 28E+22	4.02365698788 61E+22	-5.93329729903 17E+21
-5.08874228270 93E+21	6.90542237669 17E+21	-2.10648456600 15E+21
1.46904555634 72E+21	-1.50458816935 67E+21	1.50715112559 02E+20
2.11167058634 79E+19		

JOINTS

1.000000000000 00E-09	1.800000000000 00E-08	3.000000000000 00E-08
7.000000000000 00E-08	9.000000000000 00E-08	1.100000000000 00E-07
1.700000000000 00E-07	2.800000000000 00E-07	4.000000000000 00E-07

FIT INTERVAL TOO= 1.000000000000 00E-09 TIN= 5.000000000000 00E-07

PLOT INTERVAL TB= 0. TF= 1.000000000000 00E-06

BEGINNING EXPONENTIAL PARAMETERS 1.000229485228 6E-08 3.960000000000 00E+09

END EXPONENTIAL PARAMETERS 5.935901843024 0E+02 3.200000000000 00E+07

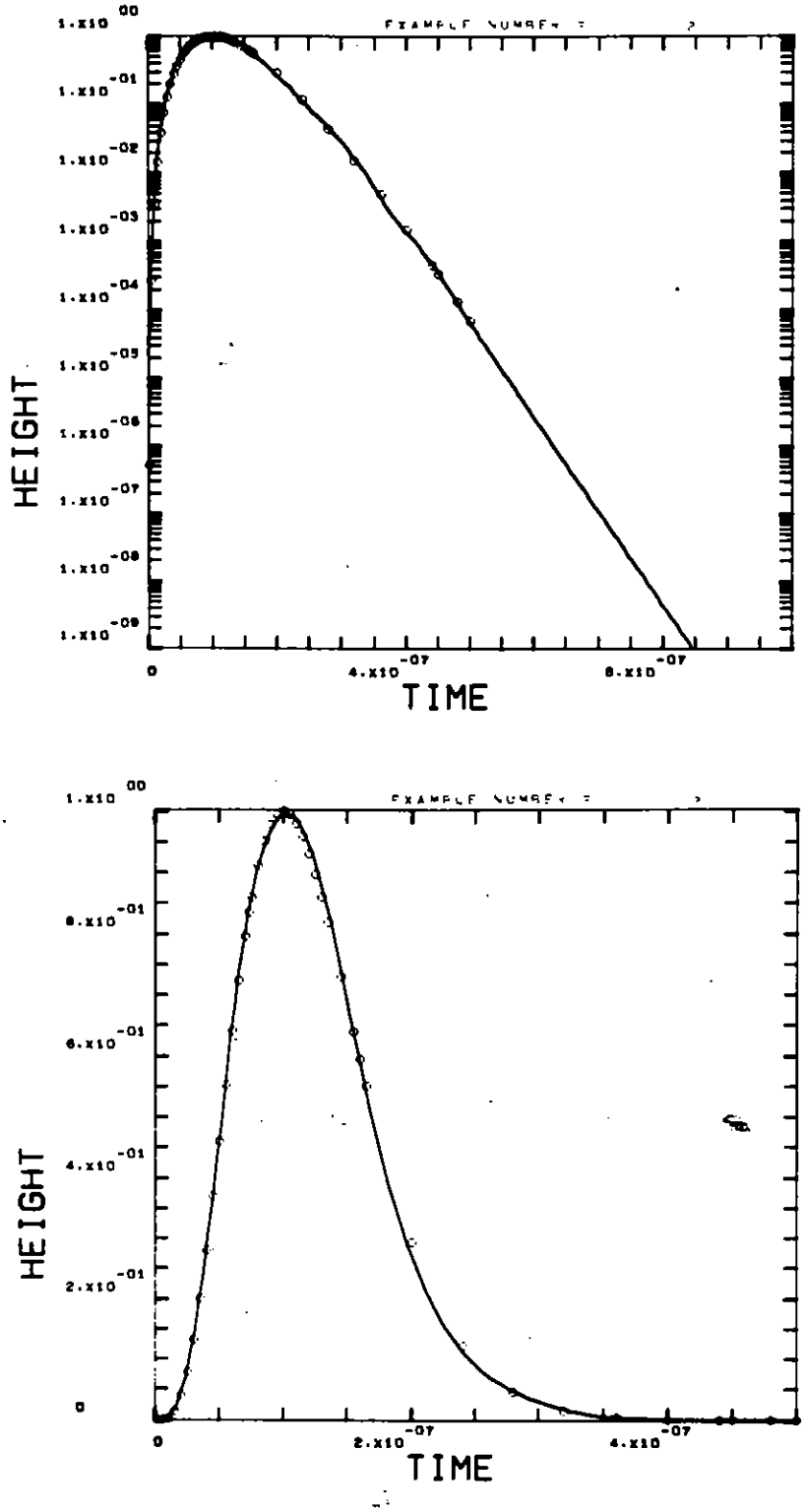

Fig. 6

Spline fit to $f_2(t)$ vs. t(sec), with end adjustments. Circles indicate data points.

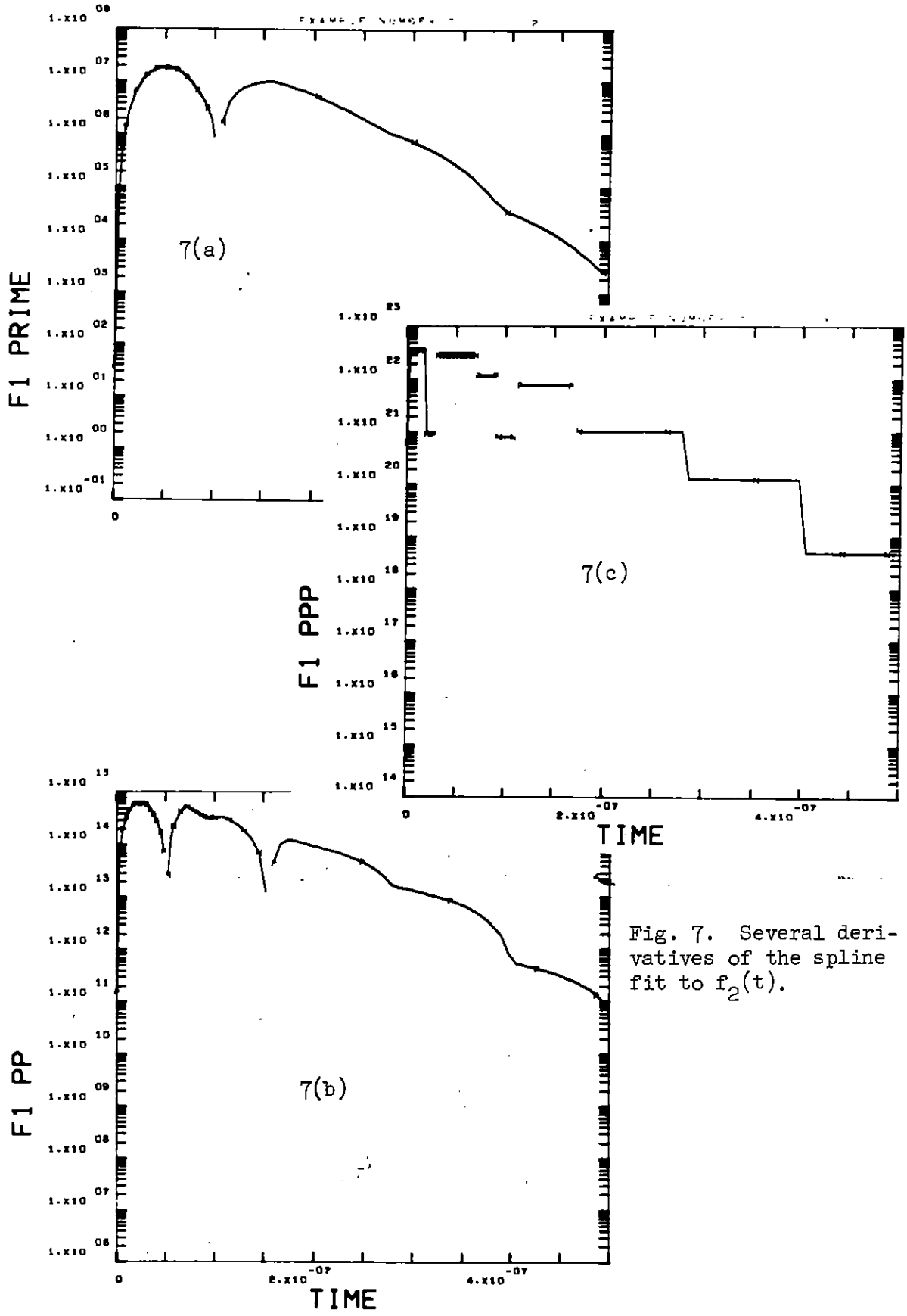

Fig. 7. Several derivatives of the spline fit to $f_2(t)$.

Success of the method is illustrated in Fig. 8 where the exact transform (from Eq.(15)) is compared with the transform calculated from the spline fit via Eq. (12) at low frequencies, and via the simpler Eq. (8) at high frequencies. Evaluation of $F(\omega)$ via Eq. (11) at low frequencies gives results in agreement with the Eq. (12) illustrated in Fig. 8 within 1%.

Figures 9 and 10 are included to indicate the $|F(\omega)|$ and its phase. Note that at high frequencies the $1/\omega^4$ variation is reasonably represented. Improvements in the agreement between the exact transform and that evaluated from the spline fit require improved fitting parameters. The reliability of the $f_2(t)$ data points could be increased; more joints could be added. Further constraints could be added. However, in applications of the method to EMP data where an exact transform is unknown, it is seldom that a sufficient number of data points (with sufficient accuracy) is available to determine the high-frequency content unambiguously. The method presented here well represents the low-frequency content of the data; it can only estimate the content at very large frequencies by a smooth fit to the given data points. The method does have the advantage that constraints may be easily used to smooth out fluctuations that are to be ignored in the data. Such fluctuations may be caused by numerical noise in computer simulations or by electrical noise in experimental measurements. A different set of constraints would retain all fluctuations present in the data and perhaps add additional ones if care is not taken. Note that in Fig. 9, discontinuities in $f'(t)$ would have forced a ω^{-2} behavior of $|F(\omega)|$ at large frequency.

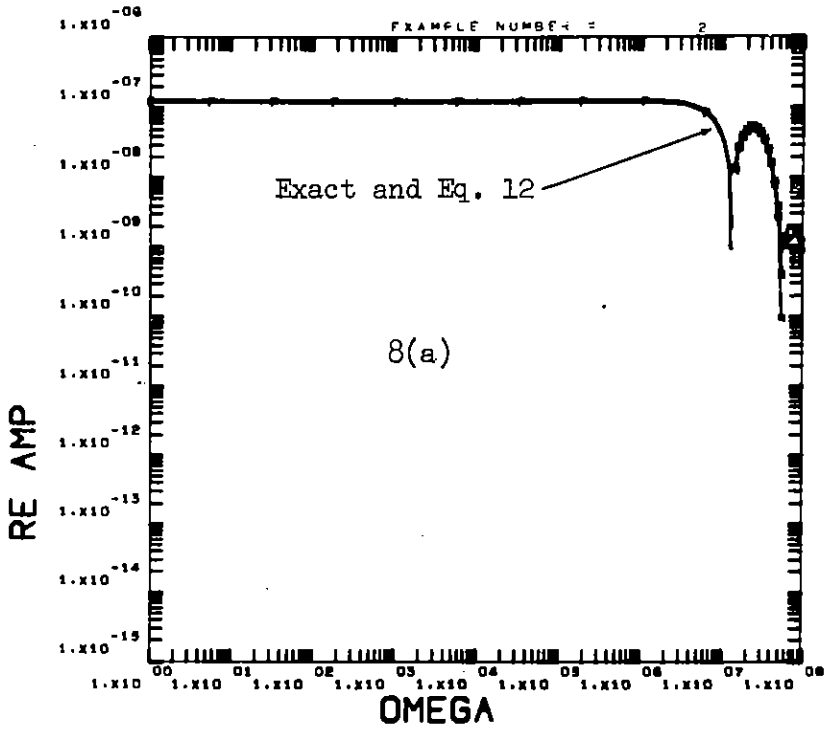

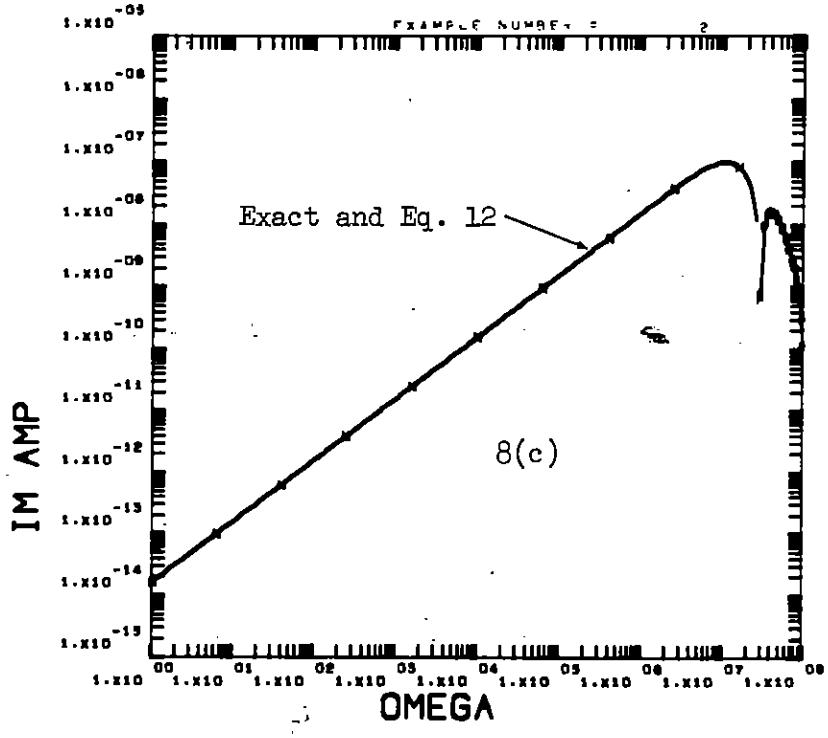

Fig. 8
Comparison of the (a, b) real and (c, d) imaginary parts of the exact transform of $f_2(t)$ and that evaluated from Eq. (8) at high frequencies. For low frequencies Eq. (12) is used.

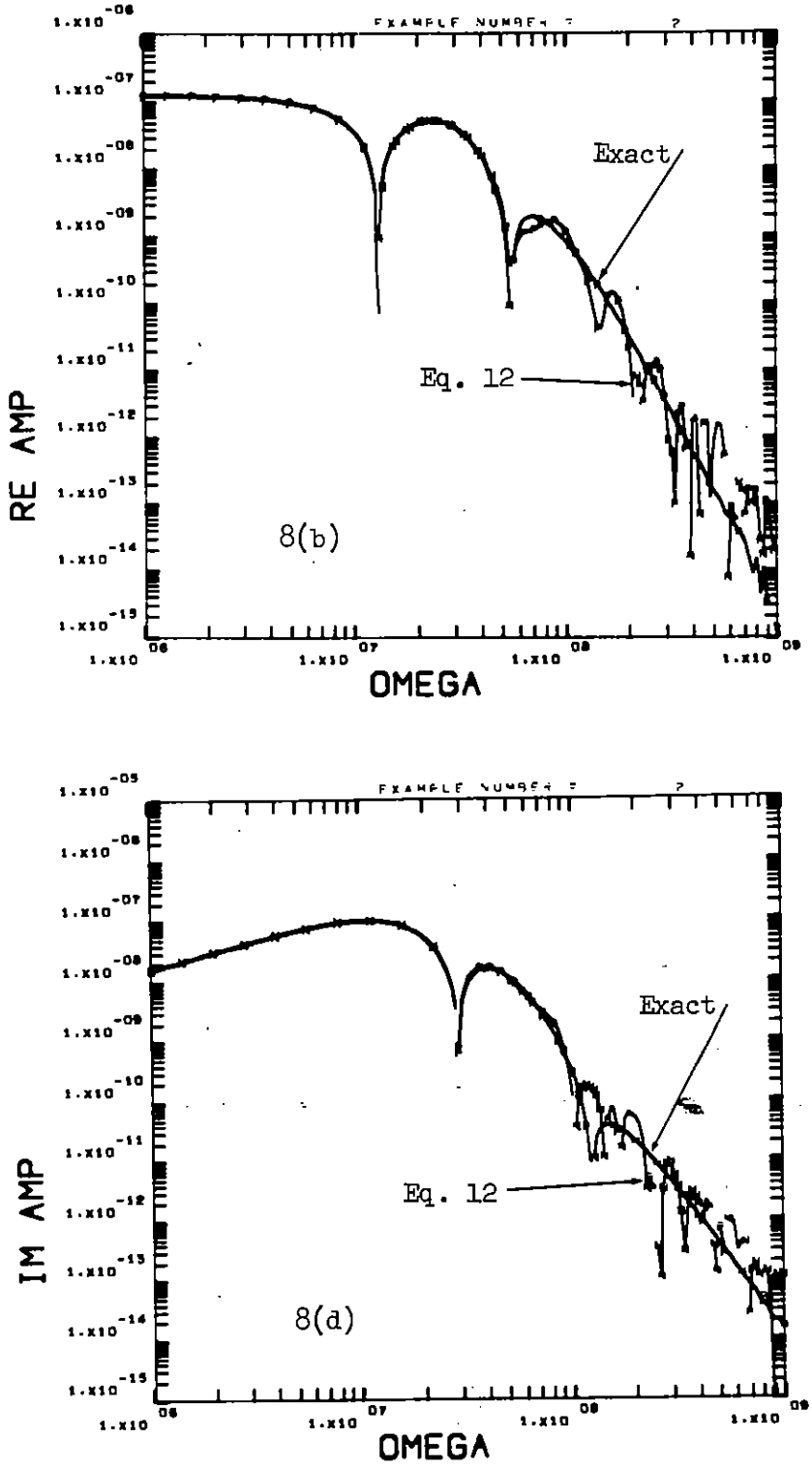

Fig. 8. Comparison of the (a, b) real and (c, d) imaginary parts of the exact transform of $f_2(t)$ and that evaluated from Eq. (8) at high frequencies. For low frequencies Eq. (12) is used.

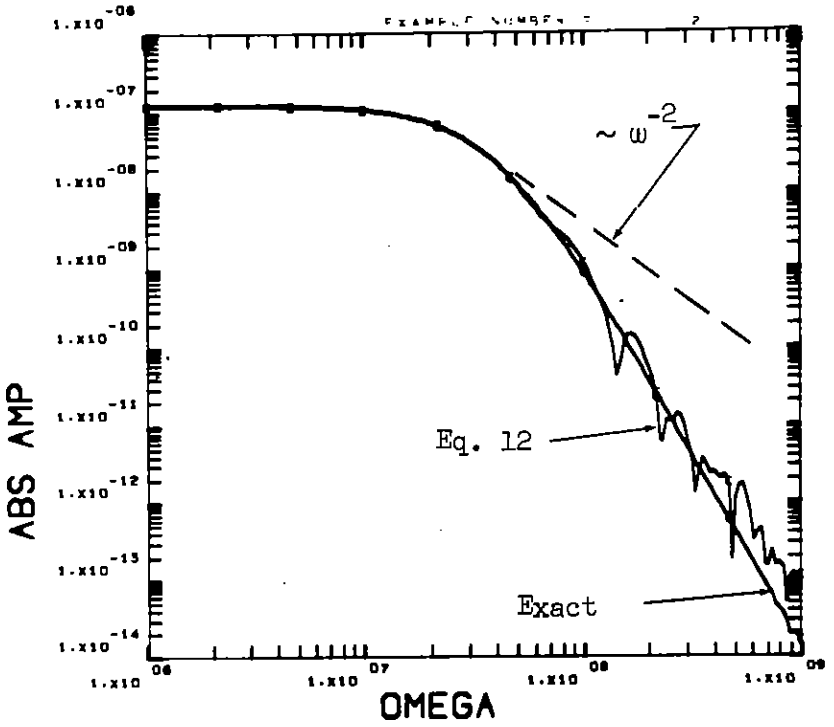

Fig. 9. The absolute value of $F(\omega)$ (sec/radian) vs. $\omega(\sec^{-1})$ for Example 2.

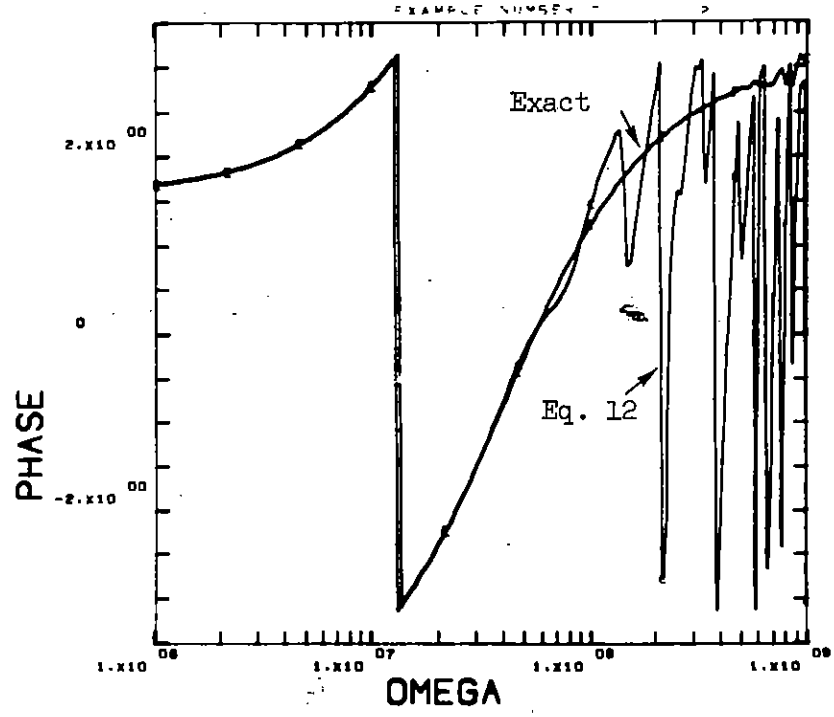

Fig. 10. The phase of $F(\omega)$ (radians) vs. $\omega(\sec^{-1})$ for Example 2. Above $\omega = 10^8$ $\sec^{-1}$ the phase is poorly represented by the particular spline fit of Example 2. The representation is excellent below the $\omega = 10^6$ $\sec^{-1}$ limit shown above.

Intentionally Left Blank

ACKNOWLEDGMENTS

This problem was started as a result of a suggestion of C. L. Longmire of Mission Research Corporation while the author was visiting MRC during the summer of 1972. The basis of the method presented was developed there. Stimulating conversations with C. L. Longmire and H. J. Longley of MRC concerning a variety of EMP problems are gratefully acknowledged. The aid of Frank Biggs and R. E. Lighthill were invaluable in efficiently learning how to apply the UNFOLD program to the problem at hand.

Intentionally Left Blank

REFERENCES

1. Electromagnetic Pulse Handbook for Missiles and Aircraft in Flight, Sandia Laboratories Report No. SC-M-71 0346, September 1972, Edited by D. E. Merewether, J. A. Cooper, and R. L. Parker.

2. G. A. Korn and T. M Korn, Mathematical Handbook for Scientists and Engineers, McGraw-Hill Book Company, New York (1968).

3. J. W. Cooley and J. W. Tukey, "An Algorithm for the Machine Calculation of Complex Fourier Series," Math. Comput. 19, 90 (1965).

4. F. Biggs and D. E. Amos, Numerical Solutions of Integral Equations and Curve Fitting, Sandia Laboratories Research Report SC-RR-71 0212, September 1971.

5. G. B. Carpenter and G. H. Price, Analysis of Data, Stanford Research Institute Report No. SRI-6-196, January 1965.

6. Handbook of Mathematical Functions, edited by M. Abramowitz and I. A. Stegun, National Bureau of Standards Applied Mathematics Series 55, December 1955.

7. D. F. Higgins, A Method for Fitting EMP Waveforms that Facilitates Calculation of the Time Derivative and Fourier Transform, Mission Research Corporation Report No. MRC-R-44, Santa Barbara, California, November 1972.